Forest Ecology and Management 315 (2014) 43–53

Contents lists available at ScienceDirect

Forest Ecology and Management

journal homepage: www.elsevier.com/locate/foreco

Evaluating spatial patterns of drought-induced tree mortality in a coastal California pine forest

Sara A. Baguskas [a,*], Seth H. Peterson [a], Bodo Bookhagen [a], Christopher J. Still [b]

[a] Department of Geography, University of California-Santa Barbara, Santa Barbara, CA 93106-4060, USA
[b] Forest Ecosystems and Society, Oregon State University, Corvallis, OR 97331, USA

ARTICLE INFO

Article history:
Received 17 September 2013
Received in revised form 6 December 2013
Accepted 18 December 2013

Keywords:
Tree mortality
Coastal fog
Drought-stress
Remote sensing
Random Forest

ABSTRACT

In a coastal, fog-influenced forest on Santa Cruz Island in southern California, we observed mortality of Bishop pine (*Pinus muricata* D.Don) trees following a brief (2 year), yet intense, drought. While anecdotal evidence indicates that drought-induced Bishop pine mortality has occurred in the past in the stand we studied, this is the first attempt to capture the spatial distribution of mortality, and begin to understand the environmental drivers underlying these events. We used high spatial resolution remote sensing data to quantify the spatial extent of tree mortality using a 1 m true color aerial photograph and a 1 m LiDAR digital elevation model. We found the highest density of dead trees in the drier, more inland margins of the forest stand. We used the Random Forest decision tree algorithm to test which environmental variables (e.g., summertime cloud frequency, solar insolation, and geomorphic attributes) would best separate live and dead tree populations. We also included tree height as a variable in our analysis, which we used as a proxy for overall tree size and potential rooting distribution. Based on the Random Forest analysis, we generated a map of the probability of survival. We found tree survivorship after drought was best explained by the frequency of summertime clouds, elevation, and tree height. Specifically, survivorship was greatest for larger trees (~8–10 m tall) in more foggy parts of the stand located at moderate elevation. We found that probability of survival was lowest at the inland extent of the stand where trees occur at the upper limit of their elevation range (~400 m). The coexistence of these main factors with other landscape variables help identify areas of suitable habitat for Bishop pines across the stand, and extend our understanding of this species' distribution.

1. Introduction

Across the western United States, widespread increases in tree mortality rates have been observed in recent decades (van Mantgem et al., 2009). Many experimental, observational, and modeling studies attribute tree mortality to drought stress in response to regional warming (Anderegg et al., 2012; Allen et al., 2010; Williams et al., 2010; Adams et al., 2009; Breshears et al., 2005; Allen and Breshears, 1998). To date, the geographical scope of studies of tree mortality in the American West has been limited to continental, montane climates (Hanson and Weltzin, 2000). Much less is known about the extent and frequency of drought-induced mortality events in coastal forests.

The maritime influence on weather and climate in coastal forests is assumed to buffer coastal ecosystems from extreme climate fluctuations, and therefore help maintain a stable distribution of species over time. However, we observed extensive mortality of a coastal pine species, Bishop pine (*Pinus muricata* D.Don), following a brief, yet intense, drought period at the southern extent of its range in California, where they are at the climatic margin that can support the species (Fischer et al., 2009; Williams et al., 2008).

Throughout the Pliocene and Pleistocene, when the California climate was considered to be more mesic compared to today, with year-round precipitation, Bishop pine, and closely related Monterey pine (*Pinus radiata*), were more widely and evenly distributed along the California coast (Raven and Axelrod, 1978). Bishop pine populations are currently restricted to a small number of stands scattered along the fog-belt of coastal California and northern Baja California (Lanner, 1999). The reduction of suitable habitat for Bishop pine (and similar coastal forests) since the late Pleistocene is attributed to the onset of xeric Mediterranean climate conditions (warmer temperatures, and reduced seasonal precipitation, occurring predominantly during the winter). However, summer precipitation from fog drip, and potentially foliar uptake of fog water (Limm et al., 2009; Limm and Dawson, 2010), is thought to enable Bishop Pines to persist along the coast and offshore islands (Raven and Axelrod, 1978).

Fog water inputs to a forest, and its effects on the water relations of trees, are spatially heterogeneous because deposition of

* Corresponding author. Tel.: +1 503 504 6854.
E-mail address: baguskas@geog.ucsb.edu (S.A. Baguskas).

0378-1127/$ - see front matter © 2013 Elsevier B.V. All rights reserved.
http://dx.doi.org/10.1016/j.foreco.2013.12.020

fog water and shading effects of fog are controlled by a variety of factors that range from the landscape to canopy scale. Fog is commonly defined as a low-stratus cloud that intercepts land. The mechanisms by which fog ameliorates the water stress of trees largely depend on their relative position to the fog layer. Shading effects, which reduce evapotranspiration, will benefit trees that are below the fog layer (Fischer et al., 2009). Plants immersed in the fog layer benefit from direct water inputs because fog droplets deposit on leaves and drip to the ground increasing shallow soil moisture (Carbone et al., 2012; Fischer et al., 2009; Corbin et al., 2005; Dawson, 1998; Ingraham and Matthews, 1995; Harr, 1982; Azevedo and Morgan, 1974; Vogelmann, 1973). Moreover, vegetation type, and canopy structure of a forest, has been shown to strongly influence fog water deposition (Ponette-Gonzalez et al., 2010; Hutley et al., 1997). For instance, direct fog water inputs decrease from the windward edge of the forest to its interior (Weathers et al., 1995), negatively impacting the water status of trees that receive less fog-water inputs in the interior (Ewing et al., 2009). Such edge effects can also impact recruitment rate of trees, and ultimately forest structure (Barbosa et al., 2010; del-Val et al., 2006). In short, the effect of fog on the growth and persistence of tree species in fog-influenced ecosystems is strongly mediated by the spatial heterogeneity of the landscape, namely topographic variation and forest structure (Uehara and Kume, 2012; Gutierrez et al., 2008; Cavelier et al., 1996; Vogelmann, 1973). Since the influence of summer cloud shading and fog drip/immersion on the moisture regime of forested ecosystems vary spatially, it is reasonable to hypothesize that the risk of drought-induced mortality in a fog-influenced forest would follow suit.

The proportion of dead Bishop pines that followed the recent drought event increased from the coast inland, and mortality was more severe at the margins of the stand. These spatial patterns seemed to coincide with modeled soil water deficit, which included the influence of fog on the water budget of the ecosystem. Specifically, Fischer et al. (2009) found that the combined effects of fog drip and cloud shading can reduce summertime drought stress up to 56% in the Bishop pine stand, and inland locations are particularly sensitive to reduced cloud shading and increased evapotranspiration compared to more coastal areas. While observations and water deficit models may infer that fog inundation and cloud shading are key climate variables explaining spatial patterns of tree mortality in this coastal forest, it is unlikely that a single environmental variable, such as fog frequency, can entirely explain the spatial patterns of tree mortality.

A suite of physical factors, such as landscape features (e.g., soil thickness and type, slope, aspect, elevation, topography, and drainage networks), can generate stress gradients across the landscape (Gitlin et al., 2006) and may explain the distribution of water stress in trees and tree mortality just as well as spatial patterns of climate (Koepke et al., 2010; Ogle et al., 2000). In addition to landscape factors, biotic factors, such as tree size, may help predict mortality within a forest stand (Floyd et al., 2009). While trees at different life stages (for which size can be proxy) may make different physiological adjustments to avoid or tolerate water stress, in general, it has been argued that larger trees with an extensive rooting distribution should be more capable of accessing stable water resources even during dry periods compared to smaller trees, and therefore be less sensitive to drought conditions (Cavender-Bares and Bazzaz, 2000; Dawson, 1996; Donovan and Ehleringer, 1994). In particular, water status of larger, adult Bishop pines is less affected by the summer dry period compared to smaller, sapling trees, which become water stressed by late-summer (S. Baguskas, *unpublished data*). Understanding how interacting environmental factors explain the spatial patterns of mortality will improve our ability to assess the vulnerability of coastal forests to drought-induced mortality in the future.

Remote sensing is a powerful tool for quantifying the spatial extent of tree mortality, which is often the first step towards elucidating patterns and processes underlying a mortality event, such as drought stress (Allen et al., 2010; Williams et al., 2010; Macomber and Woodcock, 1994), bark beetle infestation (Edburg et al., 2012; Wulder et al., 2006), and the potential impacts on regional carbon budgets (Huang and Anderegg, 2012). While many studies have quantified the spatial extent of tree mortality at regional and landscape scales using moderate-spatial (>30-m ground resolution) resolution remote sensing data (e.g., Meigs et al., 2011; Anderson et al., 2010; Fraser and Latifovic, 2005), a growing number of studies have used high-spatial (<5-m ground resolution) resolution remote sensing data to examine tree mortality at finer spatial scales in order to detect mortality of individual trees (or clusters) within a stand (e.g., Stone et al., 2012; Dennison et al., 2010; Hicke and Logan, 2009; Chambers et al., 2007; Guo et al., 2007; Coops et al., 2006; Clark et al., 2004). Developing a way to possibly make large scale estimates and predictions of tree mortality based on remotely sensed data can help land managers, who are tasked with making decisions about species and land conservation in the future, respond to a future expected to become warmer and drier.

Our research addresses the following questions: (1) What is the spatial distribution of tree mortality observed during the 2007–2009 drought period? (2) What is the correlative relationship between environmental variables, such as climate, landscape features, and tree size, and the spatial distribution of tree mortality? (3) Where is tree mortality likely to occur on the landscape during periods of drought stress?

2. Methods

2.1. Study site

This study was conducted in the westernmost and most extensive (3.6 km^2) Bishop pine stand on Santa Cruz Island (SCI, 34°N, 119°45′W), which is the largest of the northern islands in Channel Islands National Park (~250 km^2, 38 km E–W extension) located approximately 40 km south of Santa Barbara, CA (Fig. 1). The Mediterranean climate along the California coast and islands offshore is characterized by cool, rainy winters and warm, rain-free (yet foggy) summers. While rainfall is highly variable both inter- and intra-annually, on average about 80% of rain falls on SCI between December and March (Fischer et al., 2009). We observed mortality of Bishop pines during water year 2006–07 and 2008–09, when fewer than 25 cm of rain fell (median rainfall is 43 cm) (Fig. A1). In 2009, we observed peak mortality of Bishop pine trees in the field based on the high number of tree canopies with red foliage, and we found that no other plant species exhibited a mortality response like the Bishop pines did.

The Bishop pine stand that we studied exists on complex and rugged terrain ranging from sea level to just over 400 m in elevation. Bishop pines are almost entirely restricted to the wetter, cooler north-facing slopes. There are only a few scattered clusters of trees that exist on the drier south-facing slopes, and those tend to occur in drainages. Steep ridges rise from the Santa Cruz Island fault that runs E–W through the central part of the island. There is a stark ecological and geographical difference between the northern and southern sections of the island. The northern half of the island is composed of Santa Cruz Island volcanics and is sparsely vegetated compared to the southern half, which is mostly metamorphic in origin and supports most of the vegetation (Junak et al., 1995). The habitat for woody vegetation is considered to be more suitable at the center of the largest Bishop pine stand where the canopies are continuous relative to the margins of the

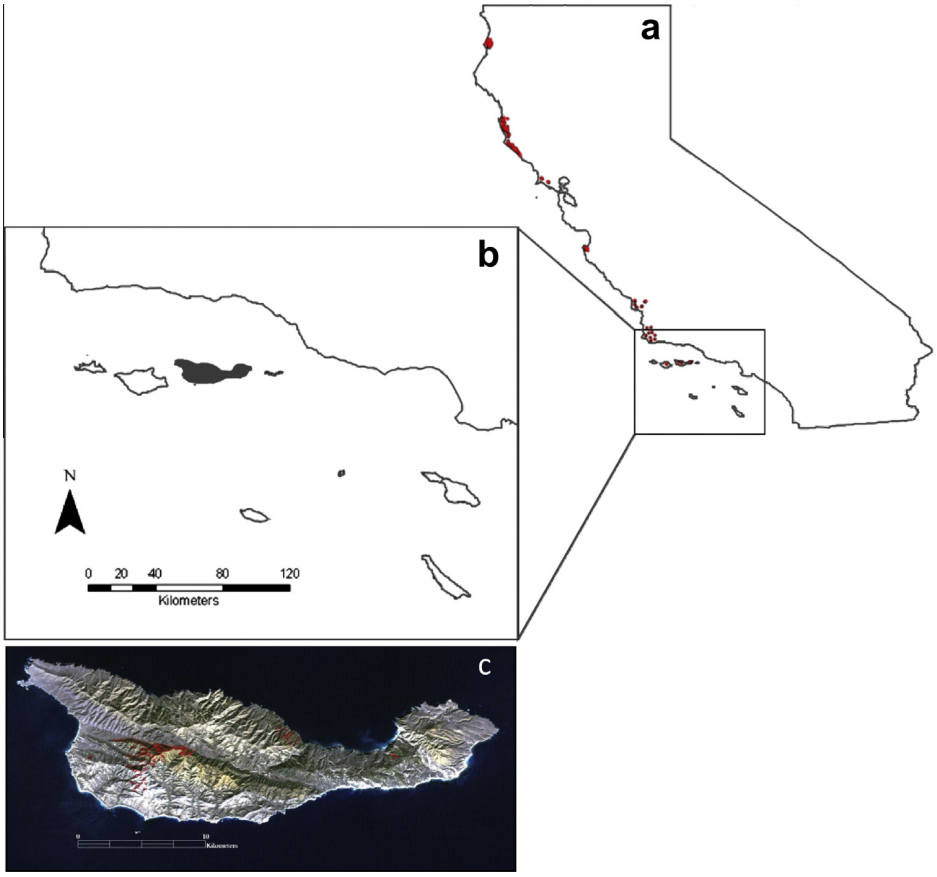

Fig. 1. (a) Study area is located on Santa Cruz Island (SCI, 34°N, 119°45′W), about 40 km off the coast of Santa Barbara in south-central California, and it supports the southernmost extent of Bishop pine trees in the United States. Other populations in California are indicated by red marks along the coastline (Lanner, 1999); (b) SCI (shaded in gray) is the largest of the islands in Channel Islands National Park; (c) Bishop pine stands on SCI are delineated with a red outline. Our study area is the westernmost and largest stand of trees. (For interpretation of the references to color in this figure legend, the reader is referred to the web version of this article.)

stand where pines are intermixed with more drought-tolerant coastal chaparral angiosperm plant species, such as Manzanita (*Arctostaphylos insularis, A. tomentosa*), Ceanothus (*Ceanothus arboreus, C. megacarpus subsp. insularis*), and Scrub Oak (*Quercus pacifica, Q. dumosa*).

2.2. Datasets

We used a variety of data sources to quantify the spatial variability and extent of tree mortality across the Bishop pine stand (Table A1). We included in our analysis Digital Orthophoto Quarter Quads (DOQQ), which are true color aerial photographs at 1-m spatial resolution, collected by the United States Geological Survey, in 2005 (pre-drought) and 2009 (post-drought). In order for us to accurately identify dead and live trees on a pixel-by-pixel basis, source images first needed to be georeferenced (i.e., aligned), with one another. The 2005 DOQQ was georeferenced to the 2009 DOQQ using 90 ground control points (GCPs) with root mean square error (RMSE) of 1.25 m. GCPs were selected from temporally invariant targets, such as road intersections. In conjunction with the DOQQ images, we used spectral information of different land cover types from an Airborne Visible Infrared Imaging Spectrometer (AVIRIS, 224 bands, 2.3 m) image collected by the Jet Propulsion Lab prior to the mortality event (7 August 2007). For the AVIRIS image, a geometric look-up table was applied to remove some of the geometric distortion for approximate georeferencing. We further improved the registration by georeferencing the AVIRIS image to the 2009 DOQQ using unambiguous reference points, such as road edges and distinct plant canopies (105 GCPs, 1.07 m RMSE).

Environmental variables used to explain the spatial patterns of tree mortality were derived from remotely sensed data (Table 1). These layers were already georeferenced. To evaluate the strength of the relationship between summertime cloud shading/fog immersion and tree mortality, we compared mortality to average summertime cloud cover frequency (Fig. 2a). Average summertime cloud cover frequency was calculated from composite MODIS (Moderate Resolution Imaging Spectroradiometer) images at 250 m collected daily at 10:30 am PST from July to September between 2000 and 2006 (Fischer et al., 2009; Williams, 2009). The 10:30 am PST overpass time of the Terra satellite captures the lingering fog from a heavy nighttime event, as the fog layer is often present until noon on SCI (Carbone et al., 2012; Fischer et al., 2009). For each MODIS pixel, a quality control classification was assigned for one of three conditions: clear sky, partial cloud cover, or total cloud cover. We determined the average fraction of days each month (i.e., frequency) when the pixels covering our study sites were classified as partially or totally cloudy using these quality classifications (Williams, 2009). In the summer, low-level marine stratus clouds are the most common cloud types on the California coast (Iacobellis and Cayan, 2013). Cloud frequency should be closely related to fog frequency, though information on elevation is required to determine whether the clouds were overhead (shading effect) or at the ground (i.e., fog immersion).

Four topographic layers (elevation, solar radiation, slope, and aspect) were included as explanatory variables. These variables

Table 1
Potential explanatory variables used in the Random Forest analyses. The Mean Decrease in Accuracy (MDA) value ranks the variables based on how well they separate live and dead tree populations in the RF analysis. The larger the MDA value, the higher ranked the variable, i.e., the greater explanatory power.

Type	Variable	Abbreviation	Data source	Spatial scale	Units	MDA
Climatic	Summertime (June–Sept.) cloud cover frequency	Clouds	MODIS	250 m	%	0.84
Topographic	Elevation	Elevation	LiDAR DEM	1 m	m	0.79
	Daily integrated summertime (June–Sept.) solar insolation	Solar insolation			MJ m^{-2}	0.72
	Slope	Slope			°	0.70
	Aspect	Aspect			°	0.63
Geomorphic	Topographic wetness index	TWI			–	0.36
	Topographic curvature	Curvature			m m^{-2}	0.28
Biotic	Vegetation height	Veg. height			m	0.81

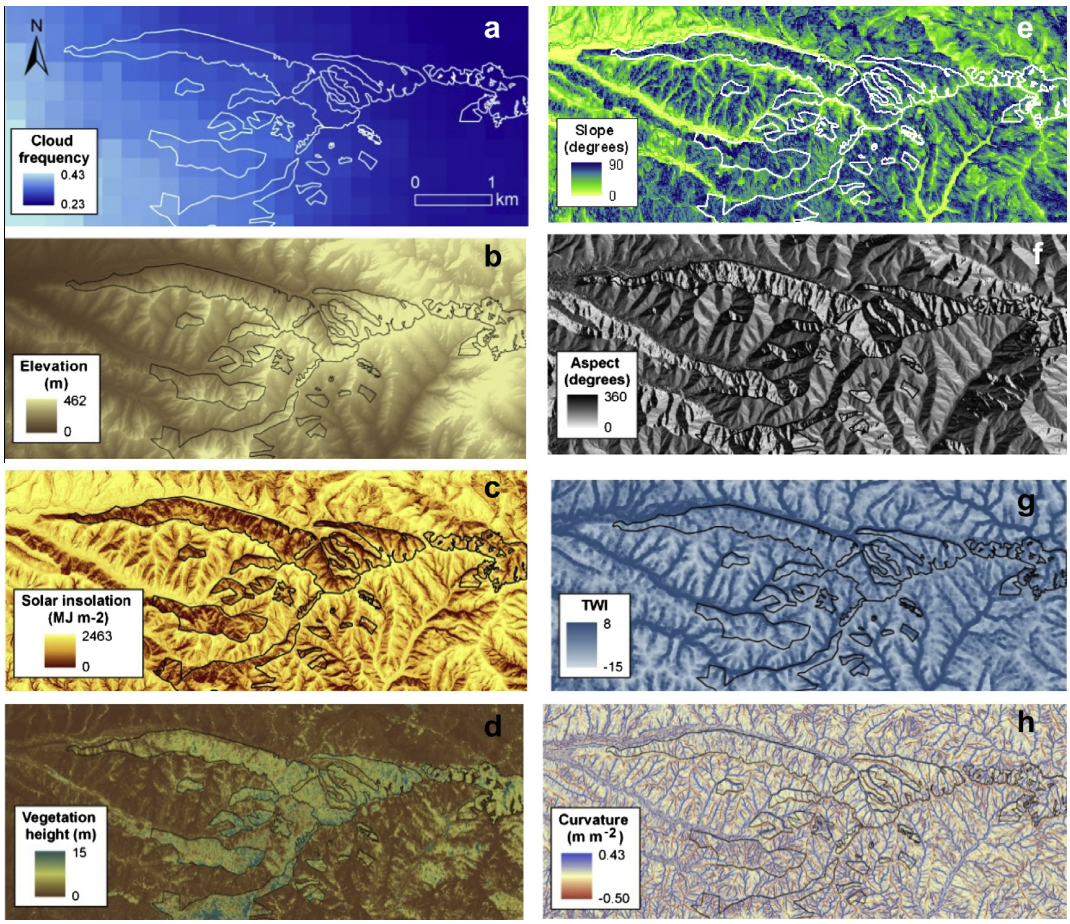

Fig. 2. Environmental layers used in the Random Forest analyses. The Bishop pine stand perimeter is delineated in each layer with a white or black line. Layers include: (a) summertime cloud frequency, (b) elevation (m), (c) solar insolation (MJ m^{-2}), (d) vegetation height (m), (e) slope (degrees), (f) aspect (degrees), (g) topographic wetness index (TWI), and (h) curvature (m m^{-2}).

exert control on the water budget of an ecosystem, such as the amount of solar radiation received by a surface (Dubayah, 1994). Topographic variables were derived from a digital elevation model (DEM) generated from a dense Light Detection and Ranging (LiDAR) point cloud collected by the USGS in January 2012. LiDAR return signals were classified into bare-earth and vegetation points and we created a regularly spaced grid at 1 m spatial resolution. The resulting DEM (Fig. 2b) has been verified in the field and found to be very robust (cf. Perroy et al., 2010, 2012). Field-based validation points were similar in 2010 and 2012, though the density of return signals was greater in 2010. From the DEM, we calculated average daytime solar radiation at the surface (i.e., insolation) for the summertime months (1 June–30 September) at 14-day intervals using standard GIS techniques (Hetrick et al., 1993) (Fig. 2c). The primary spatial variations in modeled cloud-free solar insolation for these calculations are driven by slope, aspect, and elevation. Slope and aspect (Figs. 2e and 2f, respectively) were calculated from the DEM using standard algorithms. Aspect was rotated by 180° to avoid discontinuity on north-facing slopes, where Bishop pines are most common (i.e. aspects of 1° and 359° are not different ecologically but are very different numerically). Therefore, north-facing slopes are 180°, south-facing slopes are 360°, west-facing slopes are 90°, and east-facing slopes are 270°. We used the average value for solar insolation, elevation, slope, and aspect within a 3-m radius from each tree point.

Attributes measuring the surface shape (i.e., the geomorphology of the landscape) can help characterize how topography controls and integrates hydrologic processes on a range of timescales

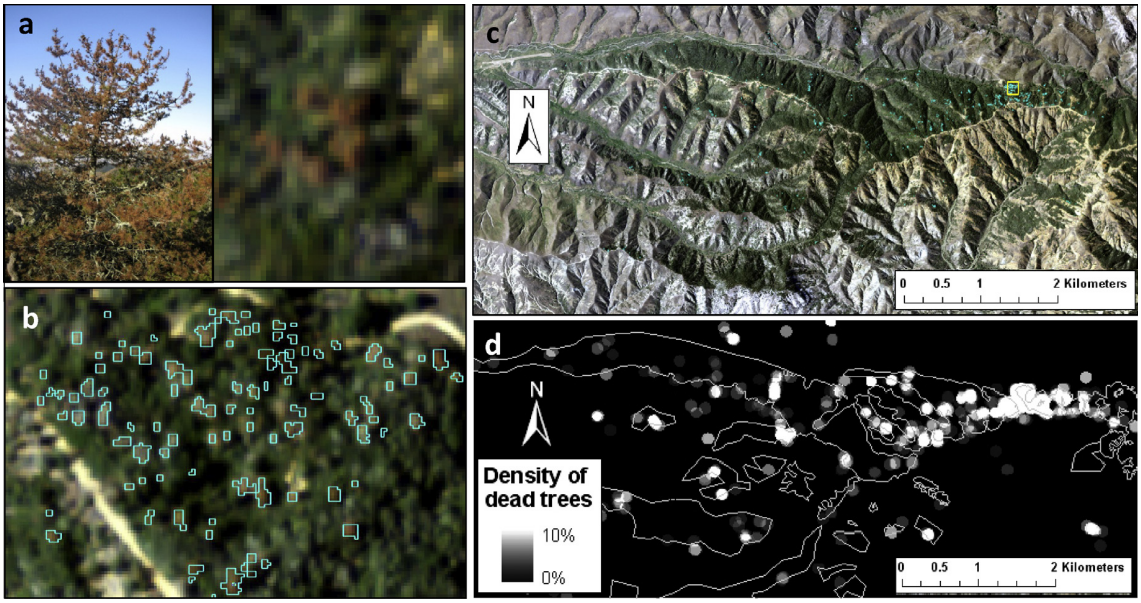

Fig. 3. (a) Photograph of a single dead Bishop pine in the field and associated red tree canopies observed in the 2009 true color aerial photo (Digital Ortho Quarter Quad from the U.S.G.S); (b) zoomed in an area highlighted by yellow box in (c) of high tree mortality in the 2009 DOQQ showing individual dead canopies delineated by cyan colored polygons; (c) showing the entire extent of westernmost Bishop pine stand where dead tree canopies (n = 871) are indicated by cyan polygons; (d) density map of dead tree canopies where white circles represent average number of dead tree canopy pixels within a 30 m radius of each dead tree. There are only circles where there is a value for tree density. Higher densities of dead trees are represented by the brighter circles. The highest density of dead tree pixels is 10%, which represents about 5–10 dead tree canopies depending on the canopy size. Stand boundaries are given by the polygons (white lines). (For interpretation of the references to color in this figure legend, the reader is referred to the web version of this article.)

(Monger and Bestelmeyer, 2006; Sørensen et al., 2006; Moore et al., 1991), and therefore strongly influences the spatial distribution of soil moisture and groundwater. We included a topographic wetness index (TWI), which describes the amount of water that potentially accumulates in every given pixel (Moore et al., 1991) (Fig. 2g). This index was calculated as (ln(upslope catchment area/slope)). We calculated the maximum values within a 4.5 m radius of each tree point to best represent the potential water accumulated at the rooting zone of the tree, which we estimated to expand at least 1–2 m beyond the tree canopy. We also included an estimate of the curvature (concavity and convexity) of the landscape, which affects the flow path of water (Ali and Roy, 2010; Gessler et al., 2000) (Fig. 2h). Curvature is the second derivative of the DEM. We calculated the average value of curvature within a 3 m radius of each tree point.

Lastly, we included a data layer of vegetation height, which we calculated from the classified LiDAR point cloud by analyzing the bare earth DEM and canopy-height DEM (Fig. 2d). Because the point of live and dead trees identified in the DOQQ may not necessarily capture the apex of the canopy in the LiDAR DEM, we calculated the maximum height for vegetation within the 3-m radius of each tree point to more accurately represent the height of each tree.

2.3. Map of tree mortality

We identified dead trees manually in the 2009 DOQQ as areas of red pixels within the Bishop pine stand (Fig. 3a). By combining this base image with the 2005 DOQQ (pre-drought), we were able to identify trees that died due to the drought period by identifying trees with red canopies in 2009 and green canopies in 2005 (Fig. 3b). We validated our remotely sensed map of mortality by measuring distances between dead tree canopies in the field and corresponding nearest dead tree canopies identified in the map. We collected location data of dead (n = 80) trees in the field using a differential GPS unit (Trimble Geoexplorer 6000 rover) in July 2010 with accuracy of <15 cm. We aimed to sample areas with low and high density of tree mortality.

2.4. Random Forest analysis

We used the Random Forest (RF) decision tree algorithm (Breiman, 2001) implemented in R (R Development Core Team 2010 version 2.12.2) to identify environmental variables that best explain the distribution of dead trees, relative to live trees, across the Bishop pine stand. The RF sample population was composed of 1740 trees, of which 869 were identified as live, and 871 as dead, *a priori*. For each of these live and dead tree points, we extracted values from the environmental variable raster datasets (Table 1), and these values were used as input to the RF analysis.

Decision trees and RF are used to uncover complex hierarchical relationships between response variables and diverse environmental variables in multivariate datasets (Michaelsen et al., 1994; Moore et al., 1991). Non-linear and non-additive relationships are learned from the data rather than explicitly modeling them (Bi and Chung, 2011; Michaelson et al., 1994). Further, they are non-parametric models, which means that variable normality and independence assumptions need not be met (Bi and Chung, 2011; Michaelson et al., 1994). Decision trees use threshold values of predictor variables to separate the response variable into more and more homogeneous groups, in our case live and dead tree populations. The RF approach aggregates the results from hundreds of individual decision trees to provide more robust predictions. Specifically, different decision trees are generated for the same data set by (1) using a sub-sample of the predictor variables at any given node (or split, based on threshold value) in the tree, and (2) using sub-samples of the response variable for training and testing each decision tree. Furthermore, values of each predictor variable are varied by ±10% and the resulting effect on classification accuracy is used to quantify variable importance through the Mean Decrease in Accuracy (MDA) score (range of 0–1) (Breiman, 2001). The greater the MDA score, the more important the variable

is in separating live and dead tree populations. While the RF analysis ranks the importance of variables, it does not indicate the nature of the relationships between explanatory variables and the dependent variable. In order to identify and illustrate the nature of these relationships, we compared the histograms of live and dead tree populations for each of these variables, and conducted a Mann–Whitney U test (R version 2.12.2) to test for significant differences between median values at the $p < 0.01$ level.

We acknowledge that some of the environmental variables used in our analysis are interdependent, e.g., slope correlates positively with solar insolation and elevation is correlated with cloudiness (Table A2). However, the use of correlated variables in RF analyses biases neither the classification output (because RF is non-parametric) nor the measure of variable importance (Peterson et al., 2012; Bi and Chung, 2011).

2.5. Predictive map of tree mortality

We created a predictive map of tree mortality using the RF results and the maps of environmental variables. Specifically, we used the R function 'yaimpute' (R version 2.12.2), which takes the 500 decision trees generated by the RF and applies them to the environmental variables. The algorithm then averages the 500 resulting predictor maps to make one final map. Areas where trees are more likely to die following drought are indicated by values closer to one, whereas trees in areas closer to zero are more likely to live. To better understand what environmental conditions characterize areas of low and high mortality during drought, we compared and contrasted average values of environmental variables at five sites that fall along a coastal inland elevation gradient established by Fischer (2007). We examined mortality risk at these sites for two reasons: (1) sites varied in their levels of probability of mortality, and (2) field data on fog-water inputs were available for these locations providing an opportunity for us to relate our remotely sensed data of environmental factors with field observations related to potential moisture availability.

3. Results

3.1. Spatial pattern of tree mortality

We were able to accurately identify mortality of nearly 900 Bishop pine trees at 1 m spatial resolution (Fig. 3b and c). To more clearly represent the spatial distribution of dead tree clusters across the stand, we generated a map of dead tree density (Fig. 3d). While there are many isolated patches of dead trees in various locations within the stand, we found the highest density of dead trees to be in the eastern, more inland margin. We assessed the accuracy of our remote sensing approach with field validation points, and found that 30% of the remotely sensed dead trees were within 10 m of the ground points ($n = 80$), and 33% of the dead trees were between 10 and 20 m (Fig. A2). In addition, visual inspection of the proximity of remotely sensed dead trees to field-based points revealed good agreement between the two datasets.

3.2. Relationship between environmental variables and tree mortality

The variables included in our RF analysis formed interacting, hierarchical relationships to distinguish dead ($n = 871$) from live ($n = 869$) tree populations within the stand. These variables, however, had different levels of importance (Table 1). Cloud frequency and elevation received a high rank by the RF analysis (Table 1, MDA: clouds = 0.84, elevation = 0.79), which suggests that the position of trees relative to the summertime stratus cloud layer is important for reducing the likelihood of mortality. Bishop pines on SCI grow along an elevation gradient that increases from the coast inland, and along this gradient, summertime cloud cover frequency decreases (Fig. A3a). We found most of the dead trees were clustered at the upper limits of the elevation range within the stand (~360–400 m), where cloud frequency was lowest (Fig. A3b), coinciding with where we observed the greatest tree mortality. Live trees spanned a broader range of elevation and cloud frequencies (Fig. A3c). In particular, most Bishop pines that died were located at or above 350 m elevation (Fig. 4a, median = 351 m) and where cloud frequency was less than 27% (Fig. 4b, median = 0.26) compared to live trees that were more frequently found below 300 m (Fig. 4a, median = 279 m) in cloudier parts of the stand (Fig. 4b, median = 0.30).

Vegetation height was found to be of roughly equal importance to cloud cover and elevation in separating live and dead trees (Table 1, MDA: veg. height = 0.81). Dead trees were significantly shorter than live trees (Fig. 4c; median dead = 7.4 m, median live = 9.0 m, $p < 0.001$). We did not find a correlation between tree height and any of the environmental factors used in our analysis; however, the spatial distribution of vegetation height indicates that taller trees dominate ridges in the southwest portion of the stand where tree mortality was minimal (Fig. 2d).

The remaining topographic variables (solar insolation, slope, and aspect) contributed to distinguishing live and dead tree populations, yet were ranked lower than cloud frequency, elevation, and vegetation height (Table 1). Nonetheless, the degree of spread and skewness in the histograms revealed subtle, but interesting differences between groups. The absolute difference in median solar insolation values between live and dead tree populations was negligible; however, live trees were normally distributed over the entire range of solar insolation values, whereas dead trees occurred more often in areas of higher solar insolation (Fig. 4d; median dead = 19.5 MJ m^{-2}, median live = 18.5 MJ m^{-2}, $p < 0.001$). Additionally, dead trees were found on more shallow slopes compared to live trees (Fig. 4e; median dead = 25°, median live = 30°). Most Bishop pines (dead or live) grew on northeast-facing slopes, yet live trees were slightly more restricted to north-facing slopes compared to dead trees (Fig. 4f; median dead = 194 °, live = 203°).

Geomorphic variables that characterize the hydrologic environment (TWI and curvature) received the lowest MDA rank relative to other variables in the RF analysis (Table 1). Both live and dead trees tended to grow in partially channelized areas of the landscape as indicated by larger, positive values of TWI (Fig. 4g). The negative curvature values for most of the trees indicate that they also grow in areas with convergent flow lines (Fig. 4h). Certainly Bishop pines grow on ridges as well, but these results suggest growing in drainages where more water accumulates is important for tree growth, especially during dry years.

Of the three environmental variables with the highest importance (clouds, elevation, and vegetation height), clouds and vegetation height showed linear relationships with probability of mortality (correlations of 0.54 and 0.48 respectively). Elevation was not linearly correlated with mortality, though the high importance value of elevation suggests a non-linear or hierarchical relationship.

3.3. Accuracy assessment for Random Forest analysis

An accuracy assessment of the RF analysis allows us to evaluate how well the RF algorithm classified live and dead trees based on the reference map we generated from the DOQQ. The accuracy of RF analysis is evaluated using a confusion matrix from which the Producer's, User's, and overall accuracy are derived (Table 2). Producer's accuracy refers to the probability that a certain land-cover

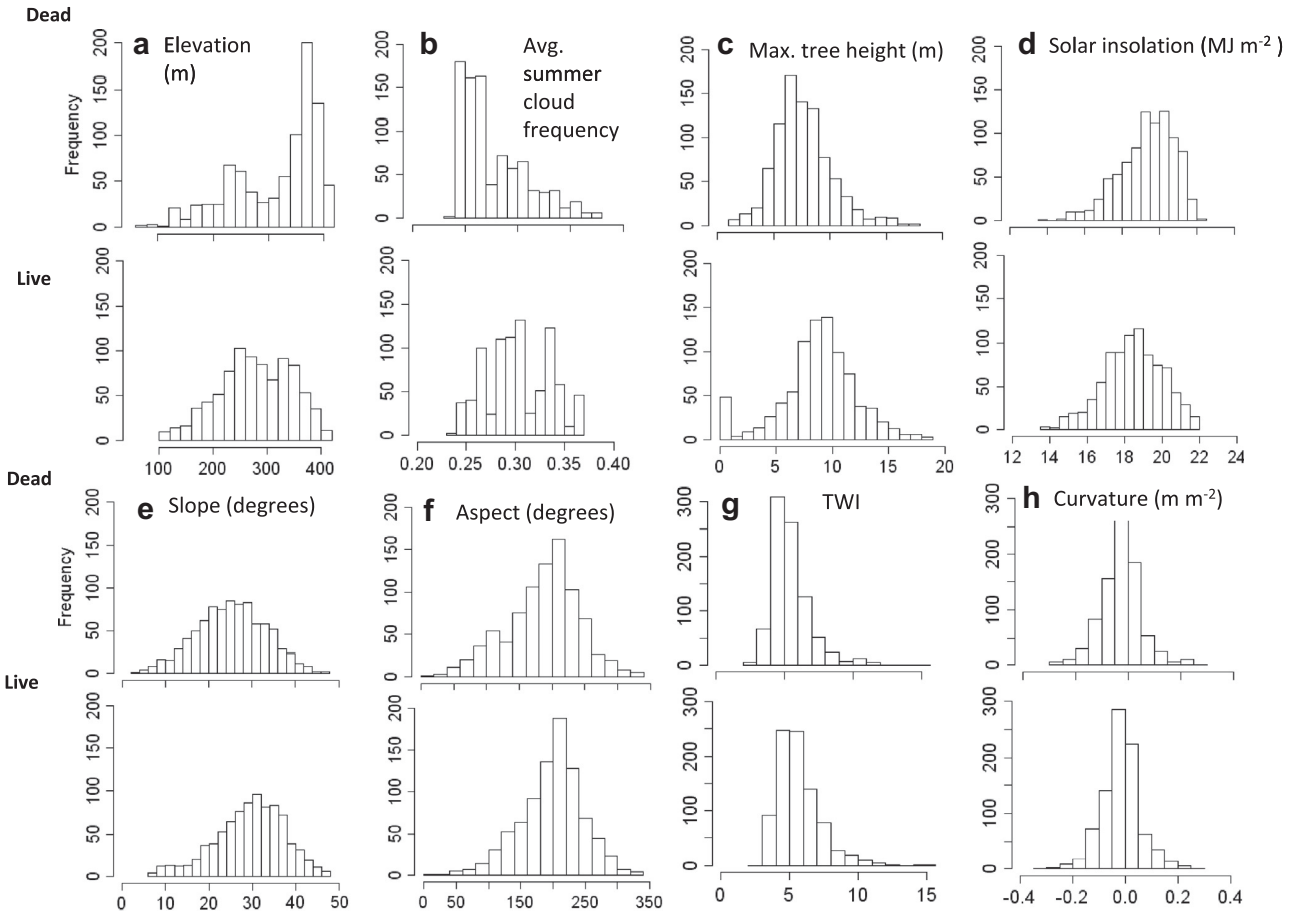

Fig. 4. Histogram of variables for dead and live tree populations. Differences between median values for live and dead tree populations differed significantly at the $p < 0.01$ level, and values are reported in text. To interpret aspect, north-facing = 180°, south-facing = 360°, west-facing = 90°, and east-facing = 270°.

category, e.g., dead trees, in the reference map was classified as such by the RF algorithm (Congalton, 1991). For example, the Producer's accuracy of dead trees was 77% because 674 pixels were modeled as 'dead' by the RF algorithm out of the total 871 identified as dead in our reference map. On the other hand, the User's accuracy refers to the probability that a pixel modeled as 'dead' is accurately modeled as dead by the RF algorithm (Congalton, 1991). For example, the User's accuracy for dead trees is 78% because 674 pixels were correctly modeled as dead out of the 863 total pixels modeled as such by the RF algorithm. The Producer's and User's accuracy results for live trees were similar to that of dead trees. Overall, the classification accuracy was high with a score of 78% (kappa 0.55). The kappa statistic incorporates misclassification information, so is a more robust measure of accuracy than overall classification accuracy (Congalton, 1991).

Table 2
Average accuracy assessment of 500 decision classification trees in Random Forest analysis.

		Reference			
		Dead	Live	Total	User's
Modeled	Dead	674	189	863	0.78
	Live	197	680	877	0.78
	Total	871	869	1740	
	Producer's	0.77	0.78		
	Overall accuracy	0.78			
	Kappa	0.55			

3.4. Predictive map of tree mortality

The predictive map identifies where trees were most vulnerable to drought-induced mortality across the Bishop pine stand given the RF results (Fig. 5). We present these results in terms of probability of mortality, where values closer to one indicate a greater probability of trees dying through a drought period. We found that the probability of mortality in the Bishop pine stand ranged from 30% to 75% and that trees growing in eastern and western margins of the stand were at greater risk of mortality (shades of red/brown) compared to the central and southwest portions of the stand (shades of blue) (Fig. 5).

We compared the probability of mortality and environmental conditions at five sites that fell along a coastal-to-inland elevation gradient for which we also had fog-water input data collected in the field (Fischer, 2007) (Table 3). The sites represent the mid-to-high values of the mortality probability scale (54–70%), and for each area we present the average values of the environmental predictor variables (Table 3). Sites were generally characterized by steep (30–34°), north-facing slopes with moderate solar insolation (17.6–18.9 MJ m^{-2}). Sites tended to be located in drainages (~−0.02–0.13 m m^{-2}) and where water accumulates (TWI, 7.9–9.1). There was greater variability in other environmental predictive variables across sites.

Site 1 is located at the western margin of the forest stand relatively close to the coast. Mortality risk is highest at this site (Table 3; probability of mortality = 70%). Of the five sites, site 1 has the highest cloud frequency (32%), yet the lowest average fog

Table 3
Average probability of tree mortality and environmental variables for the five sites indicated in Fig. 5. Sample locations were determined based on field sites for which we had data on fog-water inputs. The area of each site was approximately 20 m^2.

Site	Probability of mortality (%)	Avg. summer fog-drip (ml)[a]	Cloud cover frequency	Elevation (m)	Vegetation height (m)	Solar insolation (MJ m^{-2})	Aspect[b] (°)	Slope (°)	Curvature (m m^{-2})	TWI
1	70	597	0.32	141	5.4	17.8	208	32	0.041	8.1
2	56	938	0.28	201	9.7	17.6	186	31	−0.033	8.7
3	63	1300	0.26	423	7.8	18.9	115	30	0.076	9.2
4	64	1889	0.24	390	6.0	18.0	176	34	0.128	9.1
5	54	3205	0.31	275	11.1	18.3	131	33	−0.021	7.9

[a] Fog-drip (ml) data was collected in the field at weather stations (Fischer, 2007) from May–September in 2004. We calculated average volume of fog-water inputs over these summer months.
[b] Aspect: north-facing = 180°, south-facing = 360°, west-facing = 90°, and east-facing = 270°.

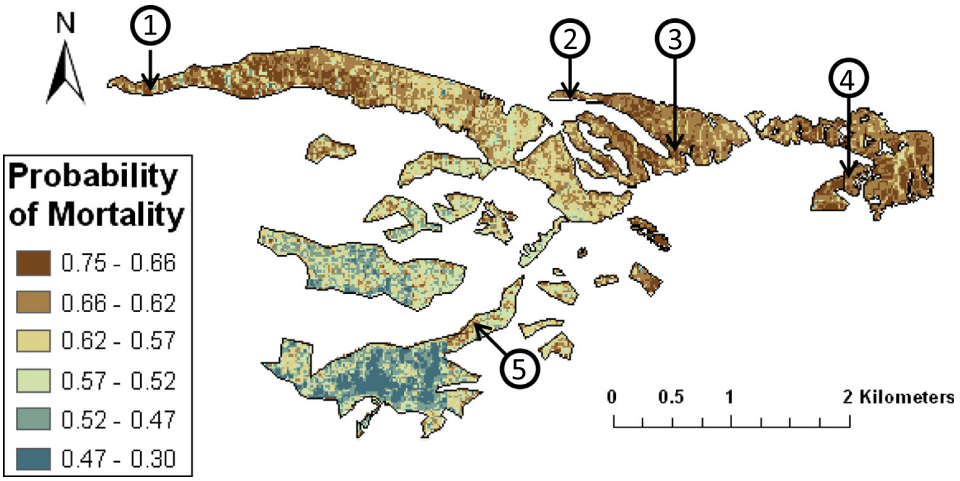

Fig. 5. Predictive map of tree mortality following drought for our study area (see Fig. 1c for reference). Bishop pine stand is delineated with a black line, and other land surface types are masked out. Red-colored areas represent areas where probability of mortality following drought is high (closer to one) compared to blue-colored areas (closer to 0). Numbered areas (1–5) are described in the text with respect to how probability of mortality relates to environmental conditions and tree height, and are included in Table 3. (For interpretation of the references to colour in this figure legend, the reader is referred to the web version of this article.)

water input over the summer (597 ml). This is likely attributed to its position below the cloud layer (elevation 141 m). Trees are shorter (5.4 m tall) than at most other sites. Site 2 is slightly higher in elevation (201 m). While less cloudy (28%) than site 1, it receives more fog-drip (938 ml) (Table 3). Trees are relatively tall (9.7 m) here and mortality risk low (56%). Site 3 is at higher elevation (423 m), with the highest solar insolation (18.9 MJ m^{-2}) of all the sites. This site has moderate values of cloud cover frequency (26%), fog-drip (1300 ml), vegetation height (7.8 m), and risk of mortality (63%) relative to other sites. Site 4 is located at the far eastern margin of the Bishop pine stand, close in elevation to site 3 (390 m). Probability of mortality (64%) is also similar to that at site 3. While cloud frequency is low (24%), fog-drip (~1900 ml) exceeded that collected at most other sites. Like site 1, vegetation was relatively short (6 m). Site 5 is located in the southwest portion of the stand at moderate elevation (275 m) where cloud frequency is high (31%) and receives the most fog-drip (3205 ml). Trees are tall (11 m) and grow on northwest facing slopes (131°).

4. Discussion

4.1. Spatial patterns of tree mortality

We accurately identified approximately 900 dead Bishop pine tree clusters in the largest Bishop pine stand on SCI. While we are confident that the high-spatial resolution of the 2009 DOQQ captured larger trees with red canopies when the photo was acquired (Fig. 3b), we believe that we under-sampled smaller trees (saplings) that we know died during the 2007–2009 drought period, based on field observations. For example, the DOQQ could not have captured smaller trees growing beneath the canopy of larger trees (Meentemeyer et al., 2008), or simply canopies too small to be detected at 1-m spatial resolution, e.g., sub-meter diameter or seedlings. Furthermore, we observe that there were smaller trees that died, or were very close to dead tree canopies, based on the vegetation height data derived from the LiDAR dataset (Fig. 4c), which has much higher precision compared to an aerial photo.

The discrepancy between field-validation points and the remotely sensed trees (Fig. A2) was likely attributed to the temporal disconnect between when we identified dead trees remotely (June 2009) and when we collected validation points (July 2010). Because many dead trees that expressed red needles in 2009 had lost their needles by July 2010, we could not identify in the field exactly which trees we identified in our remotely sensed map of mortality. Despite these shortcomings, the techniques used to identify dead trees were robust, and feel that we captured the majority of the trees that died in response to drought.

4.2. Environmental controls on tree mortality

Our study demonstrates that there is an inverse relationship between drought-induced mortality of Bishop pines and the occurrence of summertime clouds along a coastal inland elevation gradient on SCI. The spatial clustering of dead trees in the eastern, and more inland, margin of the stand is consistent with predictions from previous research. Fischer et al. (2009) characterized this area

as marginal habitat for Bishop pine based on higher modeled soil water deficit, which incorporated the cloud frequency variables used in our analysis, as well as fog water volumes collected from the field. The occurrence of fog is spatially heterogeneous, thus the strength of its impact on reducing water stress and supporting tree growth depends on how it interacts with other landscape and forest elements, such as canopy height.

The vegetation height dataset derived from the 1-m LiDAR DEM provided us with a unique opportunity to address how characteristics of vegetation interact with climatic and landscape variables. We found that larger trees (>8 m tall) that occurred in cloudier, and thus foggier, areas (~30% summertime cloud frequency, Figs. 2a and 3d) had high survivorship following drought. This agrees with previous research that showed Bishop pines had higher summertime growth rates in the cloudier portion of the stand compared to trees that grow further inland and at higher elevation (Carbone et al., 2012). The positive relationship between fog frequency, tree size, and survivability could be explained by the fact that larger trees having a greater capacity to intercept fog and generate fog drip to the soil, which can significantly offset the effects of drought stress and support growth even during low rainfall years (Carbone et al., 2012; Fischer et al., 2009). Therefore, fogginess may confer a fitness advantage over trees that grow in the less foggy, and more xeric parts of the stand (del-Val et al., 2006), which has important implications for the local distribution of trees that persist at the water-limited extent of the species range.

4.3. Environmental heterogeneity and probability of mortality

The occurrence of low-stratus clouds in the summertime is not the only factor important to the survival of Bishop pine trees during drought. Complex and subtle interactions between climate, topography, and vegetation can have large effects on plant-available water, and the suitability of habitat for growth and survival. We observed that the three main distinguishing factors between sites with the highest and lowest mortality risk (Table 3; site 1 and site 5, respectively) were elevation, volume of fog-drip, and vegetation height (Table 3). Because cloudiness was equally high at both sites (~31–32%), the large difference in fog water input is attributed to where the low-stratus clouds are intercepted by land. Based on a climatology of cloud base heights from the Santa Barbara airport, interception of low-stratus clouds is 40% more likely at sites between 240 and 280 m than at lower elevation (B. Rastogi, pers. comm). Therefore, topographic relief is necessary for cloudiness to translate to direct fog water inputs, which influences plant-available water (Fischer, 2007). In addition, trees were twice as tall at site 5 than site 1 (Table 3).

The probability of mortality was similarly low between sites 2 and 5. While these sites supported the tallest trees, they were dissimilar with respect to other environmental variables. Unlike site 5, site 2 is located at the mouth of a large drainage in the central valley on SCI, which supports cool, wet conditions compared to sites located in more exposed areas. Because ridges rise steeply from the valley floor, this site is also located on a steep, north-facing slope, which explains why solar insolation was low compared to other sites (Table 3).

The similarity in probability of mortality at sites 3 and 4 (63% and 64%, respectively) coincide with many of the environmental factors that characterize these sites. Located on ridges at the upper limit of the elevation range for Bishop pines on the island (~400 m) where cloud frequency was relatively low (24–26%) suggests that the evaporative losses may dominate at these sites. The distinguishing factor between these sites, other than measured fog-drip, is vegetation height. Trees are taller at site 3, therefore may have greater access to groundwater, which could compensate for lower fog-water inputs. Conversely, trees at site 4 are shorter, but grow on steeper slopes and are less exposed, thus buffered from drying effects.

The results of our study indicate that microhabitat conditions in the Bishop pine stand on SCI are critical for determining the survival and persistence of trees during exceptionally warm, dry periods. However, just as environmental conditions can vary widely across a forested ecosystem, many studies have demonstrated that variation in physiological adjustments of trees to stressful conditions, and differential growth patterns, are strong predictors of spatial patterns of mortality in forests (McDowell et al., 2008; Suarez et al., 2004; Wycoff and Clark, 2002; Ogle et al., 2000; Pederson, 1998; Cregg, 1994). While we did not explicitly test for variation in physiological responses or growth of Bishop pine trees in response to drought, we did find mortality risk varied among trees of different size classes. The probability of mortality was greater for shorter trees, even if the height difference was only 1–2 m (Fig. 4d). One possible explanation for this pattern could be that smaller trees have limited access to stable water reserves deeper in the soil, thus are at a disadvantage during drought periods compared to larger trees that have a greater root:shoot ratio (Suarez et al., 2004). Another interpretation of this pattern may be related to how drought has historically affected population dynamics (i.e., tree age and size structure) in the Bishop pine stand.

The most recent drought period (2007–09) was not an isolated event. Periodic droughts have affected the local distribution of Bishop pine on SCI in the past (Walter and Taha, 2000). The last major drought occurred between years 1986 and 1991, and killed off large swaths of Bishop pines across the island, particularly at the margins of the Bishop pine stands (Walter and Taha, 2000; Lyndal Laughrin, *pers. comm.*). Our results support the idea that survivorship of Bishop pine trees is compromised at the stand margins during drought (Fig. 3). However, regeneration of the pine population in these areas has not ceased (Fischer et al., 2009). The net effect of these drought cycles are even-aged cohorts dominating the stand margins. Therefore, the majority of trees we observed die after the most recent drought likely emerged following the previous drought that ended in 1991; thus, they were younger and had a shorter stature than the trees more resilient to drought stress that dominate the central and southwest parts of the stand.

4.4. Implications for management

Analyzing high-spatial resolution (1 m) aerial imagery and LiDAR remotely sensed data of tree mortality can provide more precise spatial information about the growing conditions of individual trees, or small tree clusters, and provide a more efficient approach to forest inventory (Hicke et al., 2012; Maggi and Meentemeyer, 2002). Specifically, the color infrared DOQQ used in our study clearly showed red-attack trees allowing us to delineate dead tree canopies. DOQQ imagery is available at no cost and collected 2–3 times per decade for any given local in the United States; therefore, acquiring and analyzing imagery that bookends a mortality event is feasible, allowing for a cost-effective method of inventorying forest damage. In contrast, LiDAR data is expensive and not readily available but the utility of deriving vegetation height and landscape variables was clearly demonstrated in this project.

We found RF to be a power statistical tool for analyzing a large multivariate dataset that ranked a suite of environmental variables used to predict tree mortality. This approach can be used in a variety of forest management applications that require analysis of large datasets where there may be correlation among the predictors and hierarchical and/or non-linear relationships between predictor and response variables.

This study supports the idea that low-stratus summertime clouds are important to survival of Bishop pines during drought periods at the most southern and water-limited extent of its range. However, the distribution of this species is restricted to the narrow fog-belt of California, despite the fact that precipitation is much higher further north, so fog must play a role in the more northern parts of the range as well. There is a great amount of uncertainty surrounding how the spatial and temporal variability of fog may change in the future; however, evidence suggests that fog frequency may decline in parts of the California coastline (Johnstone and Dawson, 2010), which would have negative effects on the distribution of Bishop pines and other fog-dependent species.

Acknowledgements

This work was funded by a grant from the Kearney Foundation of Soil Science. We would like to thank Carla D'Antonio, Jennifer King, and Doug Fischer for helpful comments and valuable suggestions; Ryan Perroy for assistance in the field. We thank the Nature Conservancy and the University of California Natural Reserve System for access to southwestern Santa Cruz Island.

Appendix A. Supplementary material

Supplementary data associated with this article can be found, in the online version, at http://dx.doi.org/10.1016/j.foreco.2013.12.020.

References

Adams, H.D., Guardiola-Claramonte, M., Barron-Gafford, G.A., Villegas, J.C., Breshears, D.D., Zou, C.B., Troch, P.A., Huxman, T.E., 2009. Temperature sensitivity of drought-induced tree mortality portends increased regional die-off under global-change-type drought. Proc. Natl. Acad. Sci. 106, 7063–7066.
Ali, G.A., Roy, A.G., 2010. Shopping for hydrologically representative connectivity metrics in a humid temperate forested catchment. Water Resour. Res. 46, W12544.
Allen, C.D., Breshears, D.D., 1998. Drought-induced shift of a forest-woodland ecotone: rapid landscape response to climate variation. Proc. Natl. Acad. Sci. 95, 14839–14842.
Allen, C.D., Macalady, A.K., Chenchouni, H., Bachelet, D., McDowell, N., Vennetier, M., Kitzberger, T., Rigling, A., Breshears, D.D., Hogg, E.H. (Ted)., Gonzalez, P., Fensham, R., Zhang, Z., Castro, J., Demidova, N., Lim, J.H., Allard, G., Running, S.W., Semerei, A., Cobb, N., 2010. A global overview of drought and heat-induced tree mortality reveals emerging climate change risks for forests. Forest Ecol. Manage. 259, 660–684.
Anderegg, W.R.L., Berry, J.A., Smith, D.D., Sperry, J.S., Anderegg, L.D.L., Field, C.B., 2012. The roles of hydraulic and carbon stress in a widespread climate-induced forest die-off. Proc. Natl. Acad. Sci. 109, 233–237.
Anderson, L.O., Malhi, Y., Aragão, L.E., Ladle, R., Arai, E., Barbier, N., Phillips, O., 2010. Remote sensing detection of droughts in Amazonian forest canopies. New Phytologist 187, 733–750.
Azevedo, J., Morgan, D.L., 1974. Fog precipitation in coastal California forests. Ecology, 1135–1141.
Barbosa, O., Marquet, P.A., Bacigalupe, L.D., Christie, D.A., Del-Val, E., Gutierrez, A.G., Jones, C.G., Weathers, K.C., Armesto, J.J., 2010. Interactions among patch area, forest structure and water fluxes in a fog-inundated forest ecosystem in semi-arid Chile. Funct. Ecol. 24, 909–917.
Bi, J., Chung, J., 2011. Identification of drivers of overall liking-determination of relative importances of regressor variables. J. Sens. Stud. 26, 245–254.
Breiman, L., 2001. Random forests. Machine Learning 45, 5–32.
Breshears, D.D., Cobb, N.S., Rich, P.M., Price, K.P., Allen, C.D., Balice, R.G., Romme, W.H., Kastens, J.H., Floyd, M.L., Belnap, J., Anderson, J.J., Myers, O.B., Meyer, C.W., 2005. Regional vegetation die-off in response to global-change-type drought. Proc. Natl. Acad. Sci. 102, 15144–15148.
Carbone, M.S., Williams, A.P., Ambrose, A.R., Boot, C.M., Bradley, E.S., Dawson, T.E., Schaeffer, S.M., Schimel, J.P., Still, C.J., 2012. Cloud shading and fog drip influence the metabolism of a coastal pine ecosystem. Global Change Biol. 19, 484–497.
Cavender-Bares, J., Bazzaz, F.A., 2000. Changes in drought response strategies with ontogeny in *Quercus rubra*: implications for scaling from seedings to mature trees. Oecologia 124, 8–18.
Cavelier, J., Solis, D., Jaramillo, M.A., 1996. Fog interception in montane forests across the Central Cordillera of Panama. J. Tropical Ecol. 12, 357–369.
Chambers, J.Q., Asner, G.P., Morton, D.C., Anderson, L.O., Saatchi, S.S., Espírito-Santo, F.D.B., Palace, M., Souza, C., 2007. Regional ecosystem structure and function: ecological insights from remote sensing of tropical forests. Trends Ecol. Evol. 22, 414–423.
Clark, D.B., Castro, C.S., Alvarado, L.D.A., Read, J.M., 2004. Quantifying mortality of tropical rain forest trees using high-spatial-resolution satellite data. Ecol. Lett., 52–59.
Congalton, R.G., 1991. A review of assessing the accuracy of classifications of remotely sensed data. Remote Sens. Environ. 46, 35–46.
Coops, N.C., Johnson, M., Wulder, M.A., White, J.C., 2006. Assessment of QuickBird high spatial resolution imagery to detect red attack damage due to mountain pine beetle infestation. Remote Sens. Environ. 103, 67–80.
Corbin, J.D., Thomsen, M.A., Dawson, T.E., D'Antonio, C.M., 2005. Summer water use by California coastal prairie grasses: fog, drought, and community composition. Oecologia 145, 511–521.
Cregg, B.M., 1994. Carbon allocation, gas exchange, and needle morphology of *Pinus ponderosa* genotypes known to differ in growth and survival under imposed drought. Tree Physiol. 14, 883–898.
Dawson, T.E., 1996. Determining water use by trees and forests from isotopic, energy balance and transpiration analyses: the roles of tree size and hydraulic lift. Tree Physiol. 16, 263–272.
Dawson, T.E., 1998. Fog in the California redwood forest: ecosystem inputs and use by plants. Oecologia 117, 476–485.
Dennison, P.E., Brunelle, A.R., Carter, V.A., 2010. Assessing canopy mortality during a mountain pine beetle outbreak using GeoEye-1 high spatial resolution satellite data. Remote Sens. Environ. 114, 2431–2435.
del-Val, E., Armesto, J.J., Barbosa, O., Christie, D.A., Gutiérrez, A.G., Jones, C.G., Marquet, P.A., Weathers, K.C., 2006. Rain forest islands in the Chilean semiarid region: fog-dependency, ecosystem persistence and tree regeneration. Ecosystems 9, 598–608.
Donovan, L.A., Ehleringer, J.R., 1994. Water stress and use of summer precipitation in a Great Basin shrub community. Funct. Ecol. 8, 289–297.
Dubayah, R.C., 1994. Modeling a solar radiation topoclimatology for the rio grande river basin. J. Vegetation Sci. 5, 627–640.
Edburg, S.L., Hicke, J.A., Brooks, P.D., Pendall, E.G., Ewers, B.E., Norton, U., Gochis, D., Gutmann, E.D., Meddens, A.J., 2012. Cascading impacts of bark beetle-caused tree mortality on coupled biogeophysical and biogeochemical processes. Front. Ecol. Environ. 10, 416–424.
Ewing, H.A., Weathers, K.C., Templer, P.H., Dawson, T.E., Firestone, M.K., Elliott, A.M., Boukili, V.K., 2009. Fog water and ecosystem function: heterogeneity in a California redwood forest. Ecosystems 12, 417–433.
Fischer, D.T., 2007. Ecological and Biogeographic Impacts of Fog and Stratus Clouds on Coastal Vegetation, Santa Cruz Island, CA (Doctoral Disserations). University of California, Santa Barbara, CA.
Fischer, D.T., Still, C.J., Williams, A.P., 2009. Significance of summer fog and overcast for drought stress and ecological functioning of coastal California endemic plant species. J. Biogeography 36, 783–799.
Floyd, M.L., Clifford, M., Cobb, N.S., Hanna, D., Delph, R., Ford, P., Turner, D., 2009. Relationship of stand characteristics to drought-induced mortality in three Southwestern pinon-juniper woodlands. Ecol. Appl. 19, 1223–1230.
Fraser, R.H., Latifovic, R., 2005. Mapping insect-induced tree defoliation and mortality using coarse spatial resolution satellite imagery. Int. J. Remote Sens. 26, 193–200.
Gessler, P.E., Chadwick, O.A., Chamran, F., Althouse, L., Holmes, K., 2000. Modeling soil – landscape and ecosystem properties using terrain attributes. Soil Sci. Soc. Am. 64, 2046–2056.
Gitlin, A.R., Sthultz, C.M., Bowker, M.A., Stumpf, S., Paxton, K.L., Kennedy, K., Muñoz, A., Bailey, J.K., Whitham, T.G., 2006. Mortality gradients within and among dominant plant populations as barometers of ecosystem change during extreme drought. Conservation Biol. 20, 1477–1486.
Guo, Q., Kelly, M., Gong, P., Liu, D., 2007. An object-based classification approach in mapping tree mortality using high spatial resolution imagery. GIScience Remote Sens. 44, 24–47.
Gutierrez, A.G., Barbosa, O., Christie, D.A., del-Val, E.K., Ewing, H.A., Jones, C.G., Marquet, P.A., Weathers, K.C., Armesto, J.J., 2008. Regeneration patterns and persistence of the fog-dependent Fray Jorge forest in semiarid Chile during the past two centuries. Global Change Biol. 14, 161–176.
Hanson, P.J., Weltzin, J.F., 2000. Drought disturbance from climate change: response of United States forests. Sci. Total Environ. 262, 205–220.
Harr, R.D., 1982. Fog drip in the Bull Run municipal watershed, Oregon. Water Resour. Bull. 18, 785–789.
Hetrick, W.A., Rich, M.P., Barnes, F.J., Weiss, S.B., 1993. GIS-based solar radiation flux models. Am. Soc. Photogrammetry Remote Sens. Tech. Pap. 3, 132–143.
Hicke, J.A., Johnson, M.C., Hayes, J.L., Preisler, H.K., 2012. Effects of bark beetle-caused tree mortality on wildfire. Forest Ecol. Manage. 271, 81–90.
Hicke, J.A., Logan, J., 2009. Mapping whitebark pine mortality caused by a mountain pine beetle outbreak with high spatial resolution satellite imagery. Int. J. Remote Sens. 30, 4427–4441.
Huang, C.-Y., Anderegg, W.R.L., 2012. Large drought-induced aboveground live biomass losses in southern Rocky Mountain aspen forests. Global Change Biol. 18, 1016–1027.
Hutley, L.B., Doley, D., Yates, D.J., Boonsaner, A., 1997. Water balance of an Australian subtropical rainforest at altitude: the ecological and physiological significance of intercepted cloud and fog. Aust. J. Bot. 45, 311–329.
Ingraham, N., Matthews, R., 1995. The importance of fog-drip water to vegetation: Point Reyes Peninsula, California. J. Hydrol. 164, 269–285.
Iacobellis, S.F., Cayan, D.R., 2013. The variability of California summertime marine stratus: Impacts on surface air temperatures. J. Geophys. Res.: Atmos. 118, 1–18.

Johnstone, J.A., Dawson, T.E., 2010. Climatic context and ecological implications of summer fog decline in the coast redwood region. Proc. Natl. Acad. Sci. 107, 4533–4538.
Junak, S., Ayers, T., Scott, R., Wilken, D., Young, D.A., 1995. A flora of Santa Cruz Island. Santa Barbara Botanical Garden, Santa Barbara, California.
Koepke, D.F., Kolb, T.E., Adams, H.D., 2010. Variation in woody plant mortality and dieback from severe drought among soils, plant groups, and species within a northern Arizona ecotone. Oecologia 163, 1079–1090.
Lanner, R.L., 1999. Conifers of California. Cachuma Press, Los Olivos, CA.
Limm, E.B., Simonin, K.A., Bothman, A.G., Dawson, T.E., 2009. Foliar water uptake: a common water acquisition strategy for plants of the redwood forest. Oecologia 161 (3), 449–459.
Limm, E.B., Dawson, T.E., 2010. *Polystichum munitum* (Dryopteridaceae) varies geographically in its capacity to absorb fog water by foliar uptake within the redwood forest ecosystem. Am. J. Bot. 97 (7), 1121–1128.
McDowell, N., Pockman, W.T., Allen, C.D., Breshears, D.D., Cobb, N., Kolb, T., Plaut, J., Sperry, J., West, A., Williams, D.G., Yepez, E.A., 2008. Mechanisms of plant survival and mortality during drought: why do some plants survive while others succumb to drought? New Phytologist 178, 719–733.
Macomber, S.A., Woodcock, C.E., 1994. Mapping and monitoring conifer mortality using remote sensing in the lake tahoe basin. Remote Sens. Environ. 266, 255–266.
Maggi, K., Meentemeyer, R.K., 2002. Landscape dynamics of the spread of sudden oak death. Photogrammetric Eng. Remote Sens. 68, 1001–1009.
Meigs, G.W., Kennedy, R.E., Cohen, W.B., 2011. A Landsat time series approach to characterize bark beetle and defoliator impacts on tree mortality and surface fuels in conifer forests. Remote Sens. Environ. 115, 3707–3718.
Meentemeyer, R.K., Rank, N.E., Shoemaker, D.A., Oneal, C.B., Wickland, A.C., Frangioso, K.M., Rizzo, D.M., 2008. Impact of sudden oak death on tree mortality in the Big Sur ecoregion of California. Biol. Invasions 10, 1243–1255.
Michaelsen, J., Schimel, D.S., Friedl, M.A., Davis, F.W., Dubayah, Ralph C., 1994. Regression tree analysis of satellite and terrain data to guide vegetation sampling and surveys. J. Vegetation Sci. 5, 673–686.
Monger, H., Bestelmeyer, B., 2006. The soil-geomorphic template and biotic change in arid and semi-arid ecosystems. J. Arid Environ. 65, 207–218.
Moore, D.M., Lees, B.G., Davey, S.M., 1991. A new method for predicting vegetation distributions using decision tree analysis in a geographic information system. Environ. Manage. 15, 59–71.
Ogle, K., Whitham, T.G., Cobb, N.S., 2000. Tree-ring variation in pinyon predicts likelihood of death following severe drought. Ecology 81, 3237–3243.
Pederson, B.S., 1998. The role of stress in the mortality of Midwestern oaks as indicated by growth prior to death. Ecology 79, 79–93.
Perroy, R.L., Bookhagen, B., Asner, G.A., Chadwick, O.A., 2010. Comparison of gully erosion estimates using airborne and ground-based LiDAR on Santa Cruz Island, California. Geomorphology 118, 288–300.
Perroy, R.L., Bookhagen, B., Chadwick, O.A., Howarth, J.T., 2012. Holocene and anthropocene landscape change: arroyo formation on Santa Cruz Island, California. Ann. Assoc. Am. Geographers 102, 1229–1250.
Peterson, S.H., Franklin, J., Roberts, D.A., van Wagtendonk, J.W., 2012. Mapping fuels in Yosemite National Park. Can. J. Forest Res. 43, 7–17.
Ponette-Gonzalez, A.G., Weathers, K.C., Curran, L.M., 2010. Water inputs across a tropical montane landscape in Veracruz, Mexico: synergistic effects of land cover, rain and fog seasonality, and interannual precipitation variability. Global Change Biol. 16, 946–963.
Raven, P.H., Axelrod, D.I., 1978. Origin and Relationships of the California Flora. University of California Press, Berkeley, CA.
Sørensen, R., Zinko, U., Seibert, J., 2006. On the calculation of the topographic wetness index: evaluation of different methods based on field observations. Hydrol. Earth Syst. Sci. 10, 101–112.
Stone, C., Penman, T., Turner, R., 2012. Managing drought-induced mortality in *Pinus radiata* plantations under climate change conditions: a local approach using digital camera data. Forest Ecol. Manage. 265, 94–101.
Suarez, M.L., Ghermandi, L., Kitzberger, T., 2004. Factors predisposing episodic drought-induced mortality in *Nothofagus*-site, climatic sensitivity and growth trends. J. Ecol. 92, 954–966.
Uehara, Y., Kume, A., 2012. Canopy rainfall interception and fog capture by pinus pumila regal at Mt. Tateyama in the Northern Japan Alps, Japan. Arctic, Antarctic, Alpine Res. 44, 143–150.
van Mantgem, P.J., Stephenson, N.L., Byrne, J.C., Daniels, L.D., Franklin, J.F., Fulé, P.Z., Harmon, M.E., Larson, A.J., Smith, J.M., Taylor, A.H., Veblen, T.T., 2009. Widespread increase of tree mortality rates in the western United States. Science 323, 521–524.
Vogelmann, H.W., 1973. Fog precipitation in the cloud forests of eastern Mexico. Bioscience 23 (2), 96–100.
Walter, H.S., Taha, L.A. 2000. Regeneration of Bishop pine (*Pinus muricata*) in the absence and presence of fire: a case study from Santa Cruz Island, California. In: Browne, D.R., Mitchell, K.L., Chaney, H.W. (Eds.), Proceedings of the fifth California Islands symposium, 1999 March 29 to April 1, Santa Barbara, California. San Diego, CA, U.S. Department of the Interior, Mineral Management Service (OCS Study MMS 99–0038), pp. 172–181.
Weathers, K.C., Lovett, G.M., Likens, G.E., 1995. Cloud deposition to a spruce forest edge. Atmos. Environ. 29, 665–672.
Williams, A.P., Still, C.J., Fischer, D.T., Leavitt, S.W., 2008. The influence of summertime fog and overcast clouds on the growth of a coastal Californian pine: a tree-ring study. Oecologia 156, 601–611.
Williams, A.P., 2009. Teasing foggy memories out of Pines on the California Channel Islands using Tree-Ring width and Stable Isotope approaches (Doctoral disserations). University of California, Santa Barbara, CA.
Williams, A.P., Allen, C.D., Millar, C.I., Swetnam, T.W., Michaelsen, J., Still, C.J., Leavitt, S.W., 2010. Forest responses to increasing aridity and warmth in the southwestern United States. Proc. Natl. Acad. Sci. 107, 21289–21294.
Wulder, M.A., Dymond, C.C., White, J.C., Leckie, D.G., Carroll, A.L., 2006. Surveying mountain pine beetle damage of forests: a review of remote sensing opportunities. Forest Ecol. Manage. 221, 27–41.
Wycoff, P.H., Clark, J.S., 2002. The relationship between growth and mortality for seven co-occurring tree species in the southern Appalachian Mountains. J. Ecol. 90, 604–615.